

CONFIDENTIAL

NATIONAL AERONAUTICS AND SPACE ADMINISTRATION

TECHNICAL MEMORANDUM X-13

LOW-SPEED MEASUREMENTS OF OSCILLATORY LATERAL STABILITY

DERIVATIVES OF A MODEL OF A 60° DELTA-WING BOMBER*

By John W. Paulson

Declassified by authority of NASA
Classification Change Notices No. 64 SUMMARY
Dated ** 6/1/66

DECLASSIFIED- AUTHORITY
US 1166
DROBKA TO LEBOW MEMO DATED
APRIL 19, 1966

An investigation to determine the low-speed rolling, yawing, and sideslipping derivatives of a model of a 60° delta-wing bomber has been made in the Langley free-flight tunnel. Tests were made of the composite (pod-on) and return-component (pod-off) configurations with vertical tail on and off.

The investigation showed that, in general, there was little effect of frequency on the values of the derivatives up to an angle of attack of about 20° . There were only small differences in the rolling and yawing derivatives for the composite and return-component configurations.

INTRODUCTION

An investigation has been made to determine the low-speed rolling, yawing, and sideslipping derivatives of a model of a 60° delta-wing bomber. The airplane is powered by four pod-mounted turbojet engines. A large jettisonable pod, which carries the warhead and some fuel, is mounted under the fuselage.

The investigation included rolling and yawing oscillation tests of the composite (pod-on) and return-component (pod-off) configurations with the vertical tail on and off. Sideslipping oscillation tests were made of the return component with the vertical tail on and off.

The investigation was made over an angle-of-attack range from 0° to 40° with a deflection of 0° of all controls. The reduced-frequency parameter $\omega b/2V$ was varied from 0.046 to 0.206 in the rolling and yawing oscillation tests and from 0.10 to 0.20 in the sideslipping oscillation tests.

[REDACTED]

[REDACTED]

DEFINITIONS OF TERMS AND SYMBOLS

All velocities, forces, and moments, with the exception of lift and drag, were measured with respect to the body-axes system originating at the reference center-of-gravity position located at 25-percent mean aerodynamic chord. (See fig. 1.) The term "in-phase derivative" used herein refers to any one of the stability derivatives which are based on the forces or moments in phase with the angle of roll, yaw, or sideslip produced in the oscillatory tests. The term "out-of-phase derivative" refers to any one of the stability derivatives which are based on the forces or moments 90° out of phase with the angle of roll, yaw, or sideslip. The derivatives measured in the investigation are summarized in table I. All measurements are reduced to standard coefficient form and are presented in terms of the following symbols:

X,Y,Z	body references axes unless otherwise noted
S	wing area, sq ft
b	wing span, ft
\bar{c}	mean aerodynamic chord, ft
V	free-stream velocity, ft/sec
q	free-stream dynamic pressure, lb/sq ft
I_x	moment of inertia about longitudinal body axis, slug-ft ²
I_y	moment of inertia about lateral body axis, slug-ft ²
ω	$2\pi f$, radians/sec
f	frequency of oscillation, cycles per second
k	reduced-frequency parameter, $\omega b/2V$
α	angle of attack, deg
β	angle of sideslip, deg or radians
r	yawing velocity, radians/sec
p	rolling velocity, radians/sec
t	time, sec

DECLASSIFIED

$$\dot{\beta} = \frac{d\beta}{dt}$$

$$\dot{r} = \frac{dr}{dt}$$

$$\dot{p} = \frac{dp}{dt}$$

F_L lift, lb

F_D drag, lb

F_Y side force, lb

M_Y pitching moment, ft-lb

M_X rolling moment, ft-lb

M_Z yawing moment, ft-lb

C_m pitching-moment coefficient, $\frac{M_Y}{qS\bar{c}}$

C_l rolling-moment coefficient, $\frac{M_X}{qSb}$

C_n yawing-moment coefficient, $\frac{M_Z}{qSb}$

$$C_{l\beta} = \frac{\partial C_l}{\partial \beta}, \text{ per radian}$$

$$C_{n\beta} = \frac{\partial C_n}{\partial \beta}, \text{ per radian}$$

$$C_{Y\beta} = \frac{\partial C_Y}{\partial \beta}, \text{ per radian}$$



0317102001030

C_L lift coefficient, $\frac{F_L}{qS}$

C_D drag coefficient, $\frac{F_D}{qS}$

C_Y side-force coefficient, $\frac{F_Y}{qS}$

ϕ angle of roll, radians

ψ angle of yaw, radians

$$C_{l_r} = \frac{\partial C_L}{\partial \frac{rb}{2V}}$$

$$C_{n_r} = \frac{\partial C_n}{\partial \frac{rb}{2V}}$$

$$C_{Y_r} = \frac{\partial C_Y}{\partial \frac{rb}{2V}}$$

$$C_{l_p} = \frac{\partial C_L}{\partial \frac{pb}{2V}}$$

$$C_{n_p} = \frac{\partial C_n}{\partial \frac{pb}{2V}}$$

$$C_{Y_p} = \frac{\partial C_Y}{\partial \frac{pb}{2V}}$$

$$C_{l_{\dot{\beta}}} = \frac{\partial C_L}{\partial \frac{\dot{\beta}b}{2V}}$$



DECLASSIFIED

$$c_{n\dot{\beta}} = \frac{\partial c_n}{\partial \frac{\dot{\beta} b}{2V}}$$

$$c_{Y\dot{\beta}} = \frac{\partial c_Y}{\partial \frac{\dot{\beta} b}{2V}}$$

$$c_{l\dot{r}} = \frac{\partial c_l}{\partial \frac{\dot{r} b^2}{4V^2}}$$

$$c_{n\dot{r}} = \frac{\partial c_n}{\partial \frac{\dot{r} b^2}{4V^2}}$$

$$c_{Y\dot{r}} = \frac{\partial c_Y}{\partial \frac{\dot{r} b^2}{4V^2}}$$

$$c_{l\dot{p}} = \frac{\partial c_l}{\partial \frac{\dot{p} b^2}{4V^2}}$$

$$c_{n\dot{p}} = \frac{\partial c_n}{\partial \frac{\dot{p} b^2}{4V^2}}$$

$$c_{Y\dot{p}} = \frac{\partial c_Y}{\partial \frac{\dot{p} b^2}{4V^2}}$$

L
3
9
1

CONFIDENTIAL

0370000000
APPARATUS AND MODEL

The rotary and linear oscillation tests were conducted in the Langley free-flight tunnel. Detailed descriptions of the apparatus and methods used in deriving the data are given in reference 1. The model was sting mounted, and the forces and moments were measured about the body axes by means of a three-component internal strain-gage balance. A three-view drawing of the model is shown in figure 2, and the dimensional and mass characteristics are given in table II.

TESTS

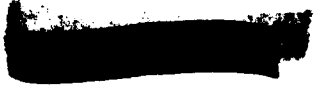
The oscillation tests were made over an angle-of-attack range from 0° to 40° with all controls at a deflection of 0° . The rolling and yawing tests were made for the composite and return-component configurations with vertical tail on and off and with the reduced-frequency parameter $\omega b/2V$ varied from 0.046 to 0.206. These tests were made for an amplitude of $\pm 10^\circ$. The sideslipping tests were made for only the return-component configuration with vertical tail on and off over a reduced-frequency-parameter range from 0.10 to 0.20. The amplitude of the oscillation in the sideslipping tests was ± 0.416 foot or $\pm 1.2^\circ$ to $\pm 2.4^\circ$.

The tests were made at a dynamic pressure of 4.77 pounds per square foot, which corresponds to an airspeed of about 63 feet per second at standard sea-level conditions and to a test Reynolds number of 970,000 based on the mean aerodynamic chord of 2.41 feet.

RESULTS

The results of this investigation are presented herein without discussion. The static longitudinal and lateral stability characteristics of the composite and return-component configurations are presented in figures 3 and 4, respectively, to afford a more convenient correlation with the data on the oscillatory derivatives.

The data for the composite and return components obtained from the rolling oscillation tests are presented in figures 5 to 12 and those from the yawing oscillation tests are presented in figures 13 to 20. The data obtained from the sideslipping oscillation tests are presented in figure 21 for the return component.



Rolling

Presented in figures 5 and 6 is the variation with frequency of the out-of-phase and in-phase derivatives, respectively, for the composite model. The derivative data for the return component are presented in figures 7 and 8. The out-of-phase and in-phase derivatives are summarized in figures 9 through 12 for the composite and return-component models in terms of the variation of the derivatives with angle of attack for constant values of the reduced-frequency parameter.

The out-of-phase derivative data (figs. 9 and 10) show that neither the pod nor the vertical tail had much effect on the derivatives and also that the effect of frequency was generally small, up to at least an angle of attack of 20° . The in-phase derivative data (figs. 11 and 12) show that there was little effect of frequency except at the higher angles of attack.


Yawing

Presented in figures 13 and 14 is the variation with frequency of the out-of-phase and in-phase derivatives, respectively, for the composite model. The derivative data for the return component are presented in figures 15 and 16. The out-of-phase and in-phase derivatives are summarized in figures 17 through 20 for the composite and return-component models in terms of the variation of the derivatives with angle of attack for constant values of the reduced-frequency parameter.

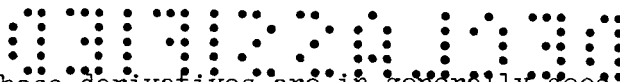
The out-of-phase derivative data (figs. 17 and 18) show that for the yawing oscillation tests there were some differences in the values of the derivatives between the composite and return-component configurations and that the vertical tail had an appreciable effect. The major effects of frequency again occurred in the higher angle-of-attack range, as in the case of the rolling oscillation data. The in-phase derivative data (figs. 19 and 20) are not greatly affected by frequency up to about an angle of attack of 20° . Comparison of these data with those of figure 4 shows that there is generally good agreement between the static data and the in-phase derivative data obtained from the oscillation tests.

Sideslipping

Presented in figure 21 is the variation with angle of attack for the out-of-phase and in-phase derivatives at constant values of the reduced-frequency parameter for the return-component configuration. These data again show that the effects of frequency on the out-of-phase derivatives are generally the greatest above an angle of attack of 20° ,



CONFIDENTIAL



and the in-phase derivatives are in generally good agreement with the static data of figure 4.

Langley Research Center,
National Aeronautics and Space Administration,
Langley Field, Va., February 26, 1959.

REFERENCE

1. Hewes, Donald E.: Low-Subsonic Measurements of the Static and Oscillatory Lateral Stability Derivatives of a Sweptback-Wing Airplane Configuration at Angles of Attack From -10° to 90° . NASA MEMO 5-20-59L, 1959.

I
3
9
1

DECLASSIFIED

TABLE I

DERIVATIVES MEASURED IN OSCILLATORY TESTS

	Rolling	Yawing	Sideslipping
In-phase derivatives	$C_{l\beta} \sin \alpha - k^2 C_{l\dot{\beta}}$ $C_{n\beta} \sin \alpha - k^2 C_{n\dot{\beta}}$ $C_{Y\beta} \sin \alpha - k^2 C_{Y\dot{\beta}}$	$C_{l\beta} \cos \alpha + k^2 C_{l\dot{r}}$ $C_{n\beta} \cos \alpha + k^2 C_{n\dot{r}}$ $C_{Y\beta} \cos \alpha + k^2 C_{Y\dot{r}}$	$C_{l\beta}$ $C_{n\beta}$ $C_{Y\beta}$
Out-of-phase derivatives	$C_{l_p} + C_{l\dot{\beta}} \sin \alpha$ $C_{n_p} + C_{n\dot{\beta}} \sin \alpha$ $C_{Y_p} + C_{Y\dot{\beta}} \sin \alpha$	$C_{l_r} - C_{l\dot{\beta}} \cos \alpha$ $C_{n_r} - C_{n\dot{\beta}} \cos \alpha$ $C_{Y_r} - C_{Y\dot{\beta}} \cos \alpha$	$C_{l\dot{\beta}}$ $C_{n\dot{\beta}}$ $C_{Y\dot{\beta}}$



03:41:29.130

TABLE II

MASS AND DIMENSIONAL CHARACTERISTICS OF A MODEL OF A 60° DELTA-WING
BOMBER USED IN THE INVESTIGATION

Weight, lb:

Composite	15.1
Return-component	16.0

Moments of inertia, slug-ft²:

Composite:

I _x	0.34
I _y	1.54

Return-component:

I _x	0.32
I _y	1.40

Wing:

Airfoil section:

Root chord	NACA 0003.46-64.069
Span station 0.22 and outboard	NACA 0004.08-63
Area (total), sq ft	6.85
Span, ft	3.79
Aspect ratio	2.1
Root chord, ft	3.61
Tip chord, ft	0
Mean aerodynamic chord, ft	2.41
Sweepback of leading edge, deg	60
Sweepforward of trailing edge, deg	10
Dihedral, deg	0
Incidence, deg	3

DECLASSIFIED

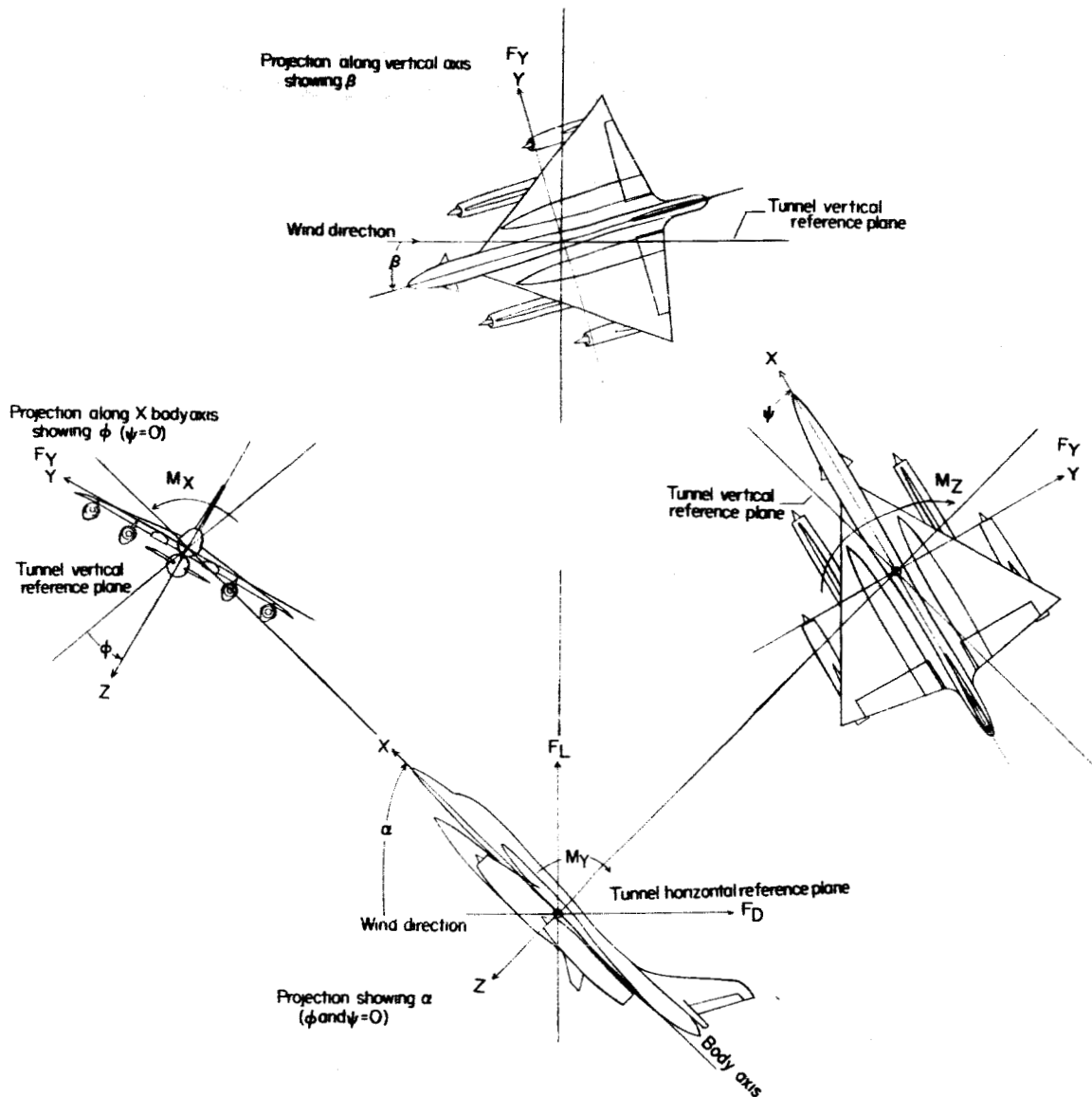


Figure 1.- Body system of axes. Arrows indicate positive directions of moments, forces, and angles. This system of axes is defined as an orthogonal system having the origin at the center of gravity, and the X-axis is in the plane of symmetry and aligned with the longitudinal axis of the fuselage. The Z-axis is in the plane of symmetry and perpendicular to the X-axis, and the Y-axis is perpendicular to the plane of symmetry.

03:71224.1030

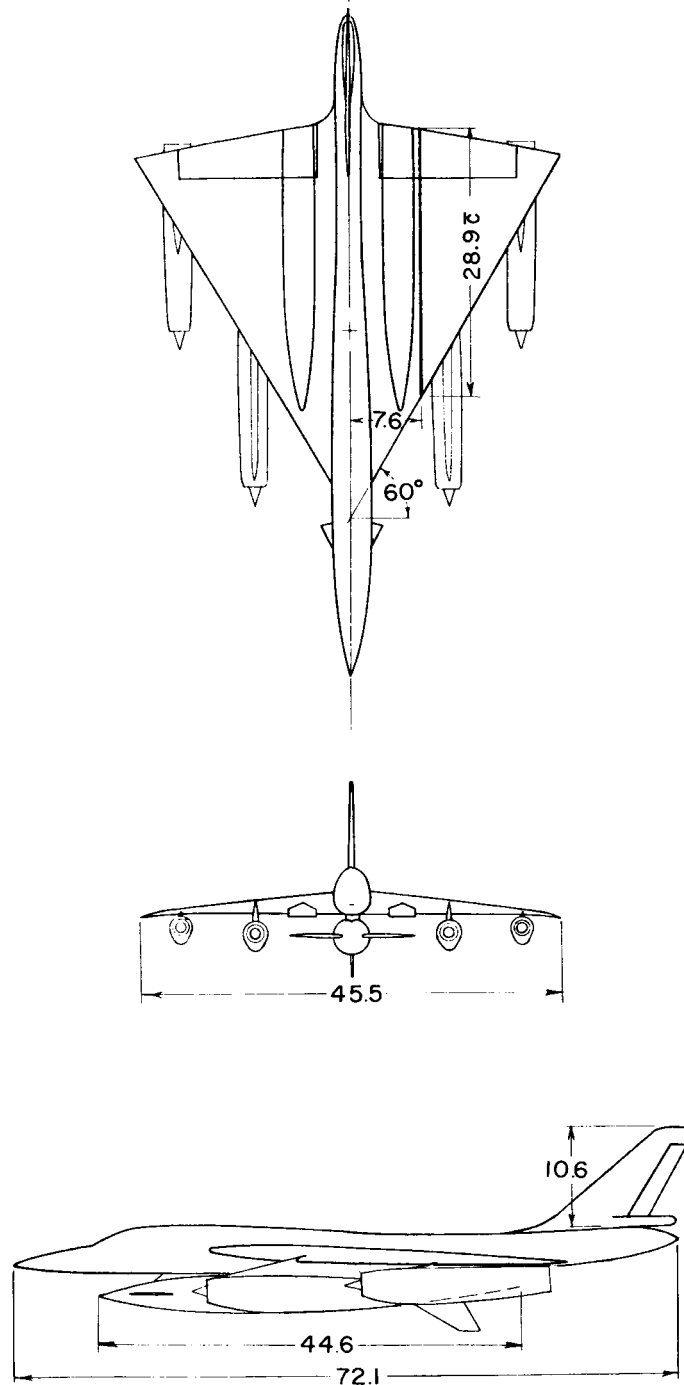


Figure 2.- Three-view drawing of model of 60° delta-wing bomber used in investigation. All dimensions are in inches.

DECLASSIFIED

○ ————— Composite
 □ — — — — — Return component

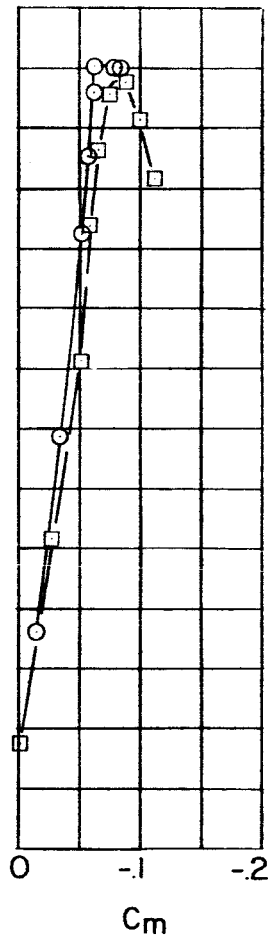
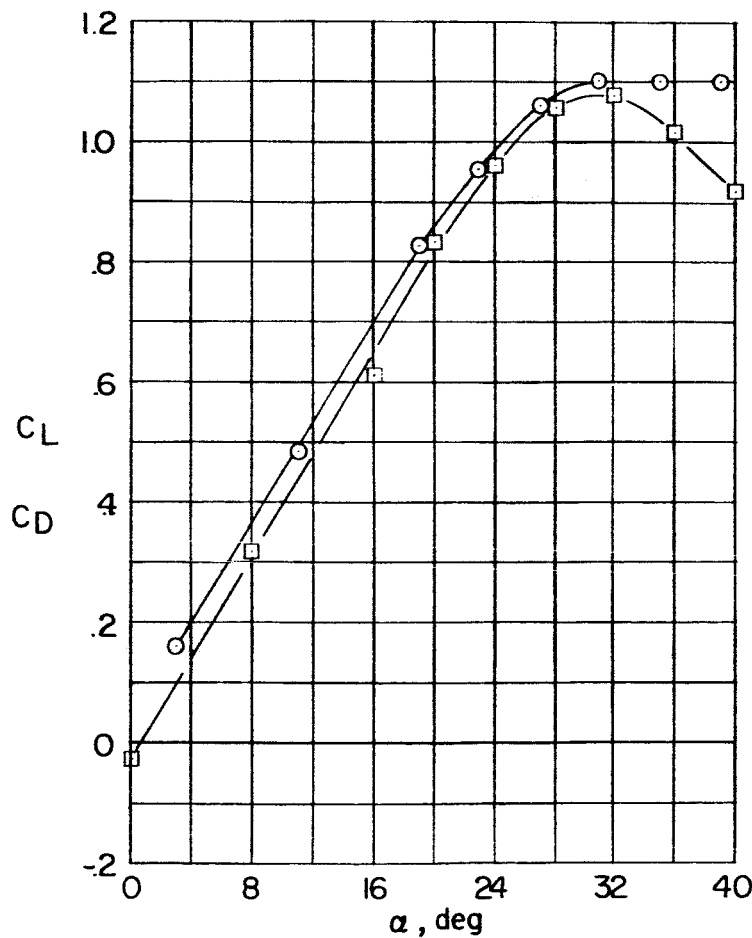
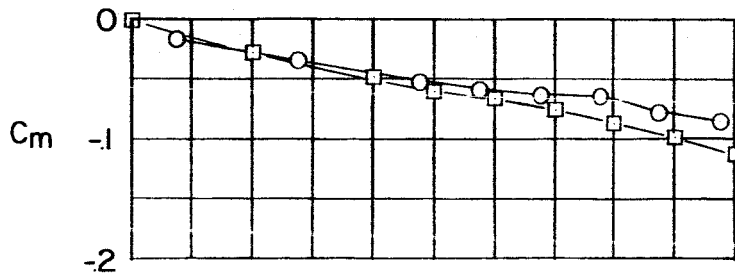


Figure 3.- Aerodynamic characteristics of models used in investigation.
 $\beta = 0^\circ$.

CONFIDENTIAL

037120041030

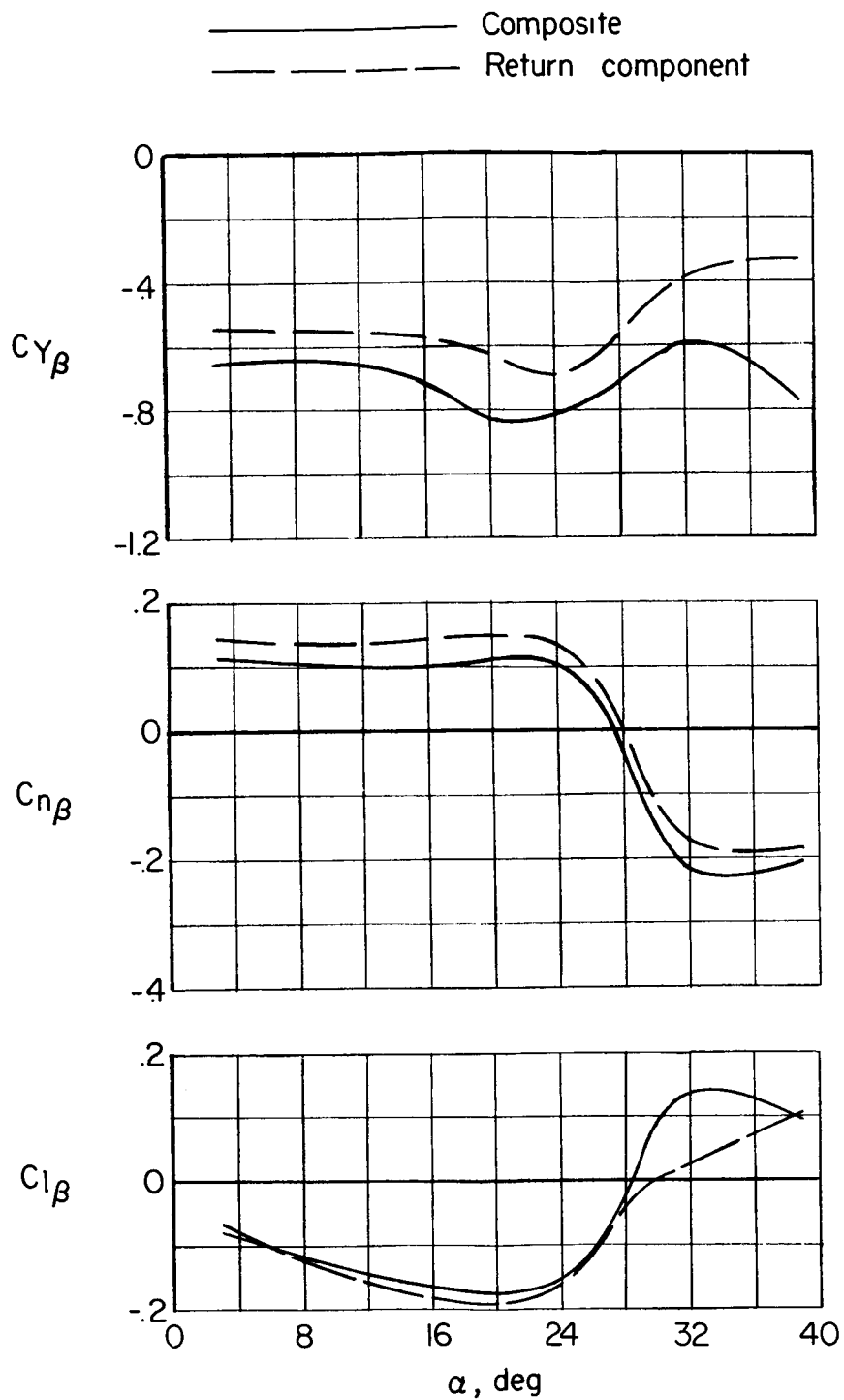


Figure 4.- Static lateral characteristics of models used in investigation.

DECLASSIFIED

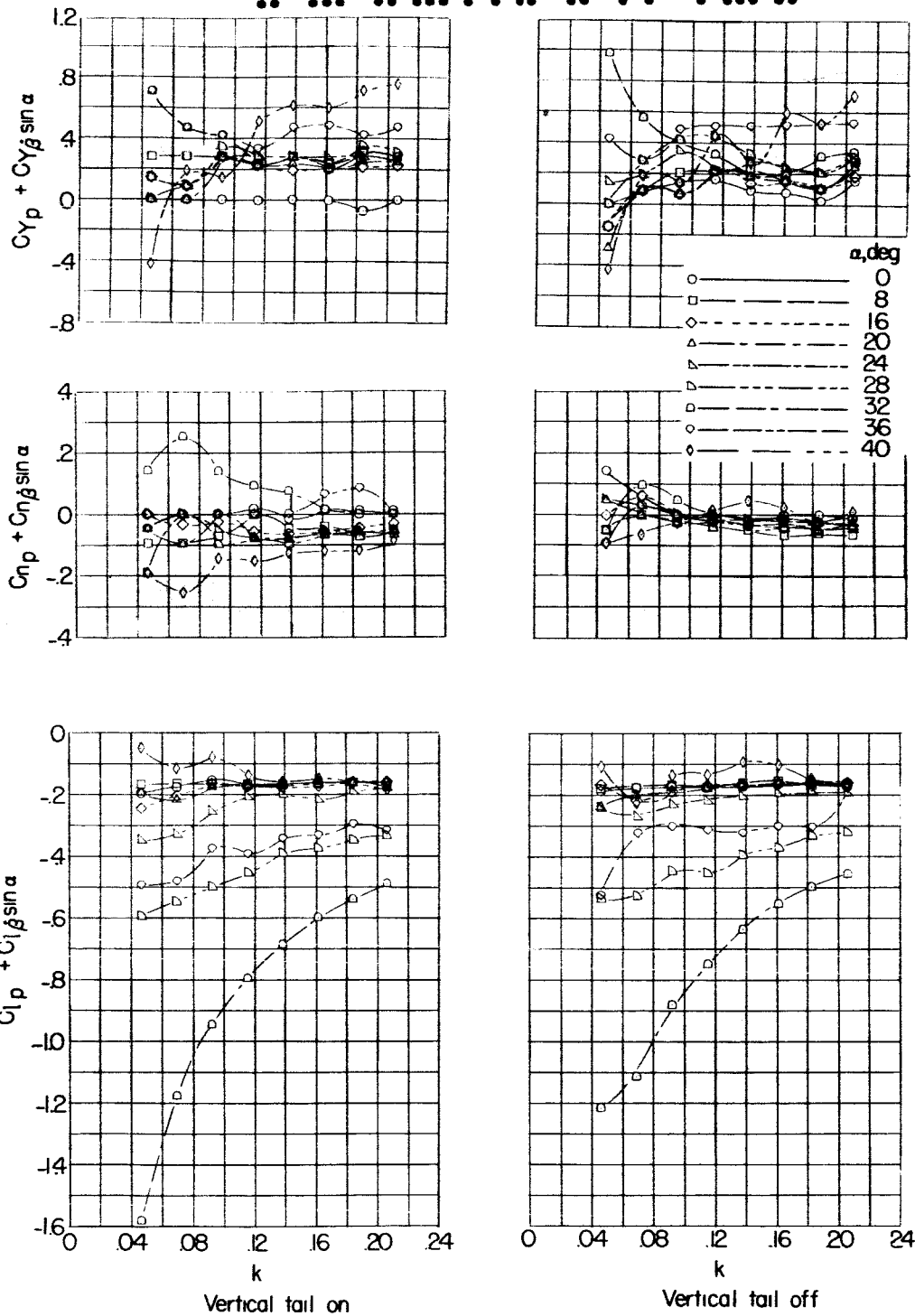


Figure 5.- Variation of out-of-phase rolling derivatives with frequency. Composite.

03713201030

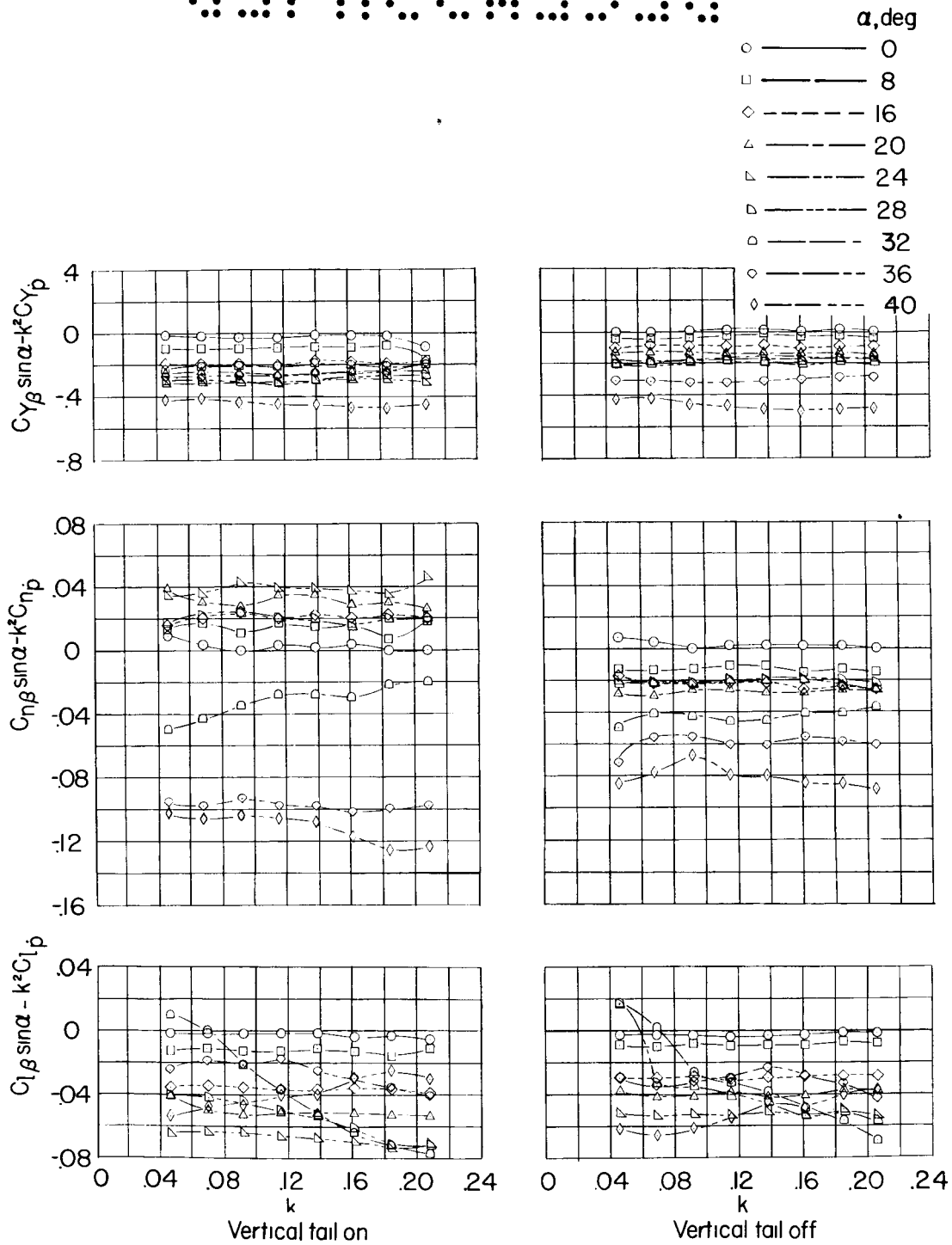


Figure 6.- Variation of in-phase rolling derivatives with frequency.
Composite.

CONFIDENTIAL

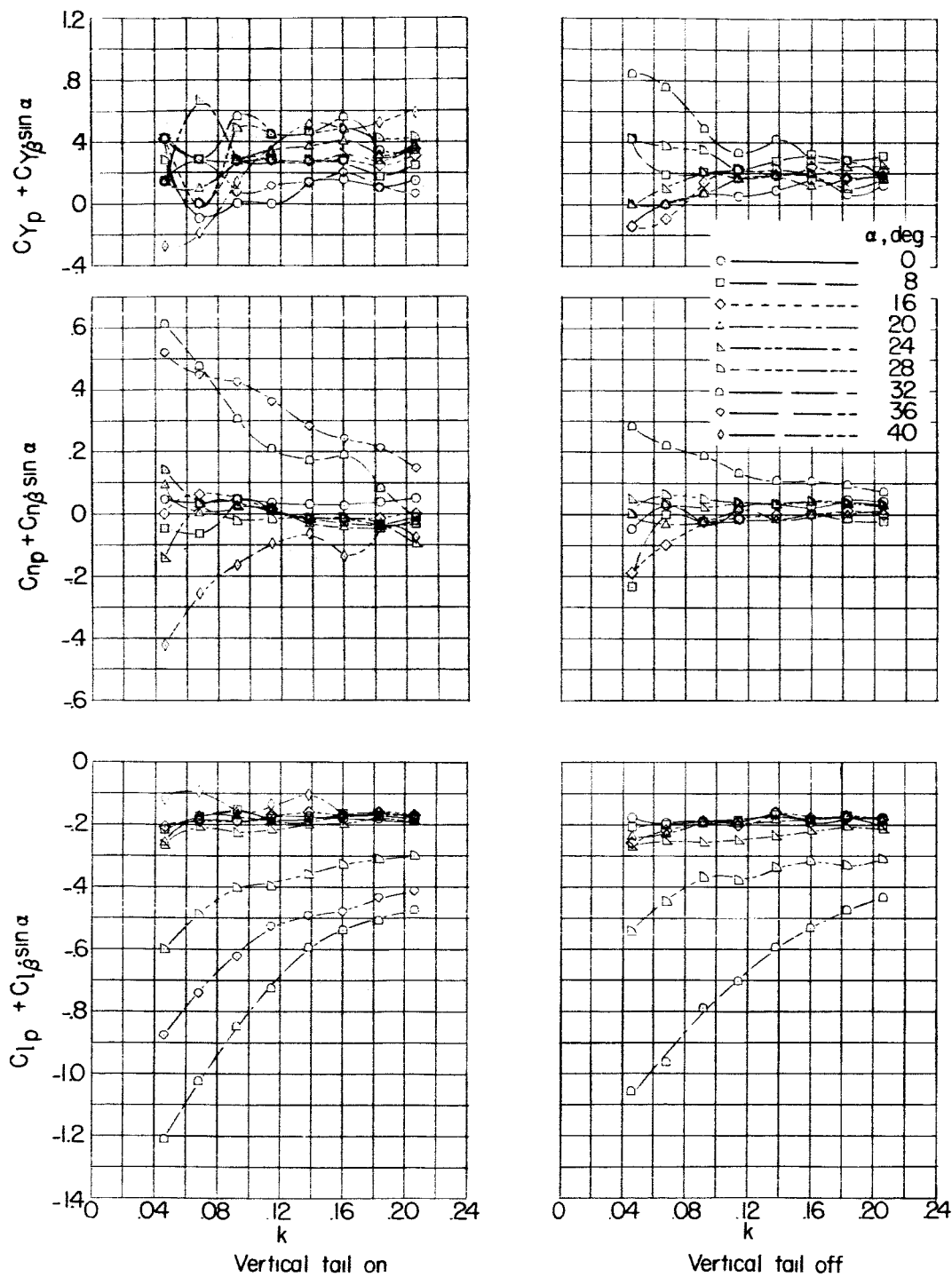


Figure 7.- Variation of out-of-phase rolling derivatives with frequency.
Return component.

CONFIDENTIAL

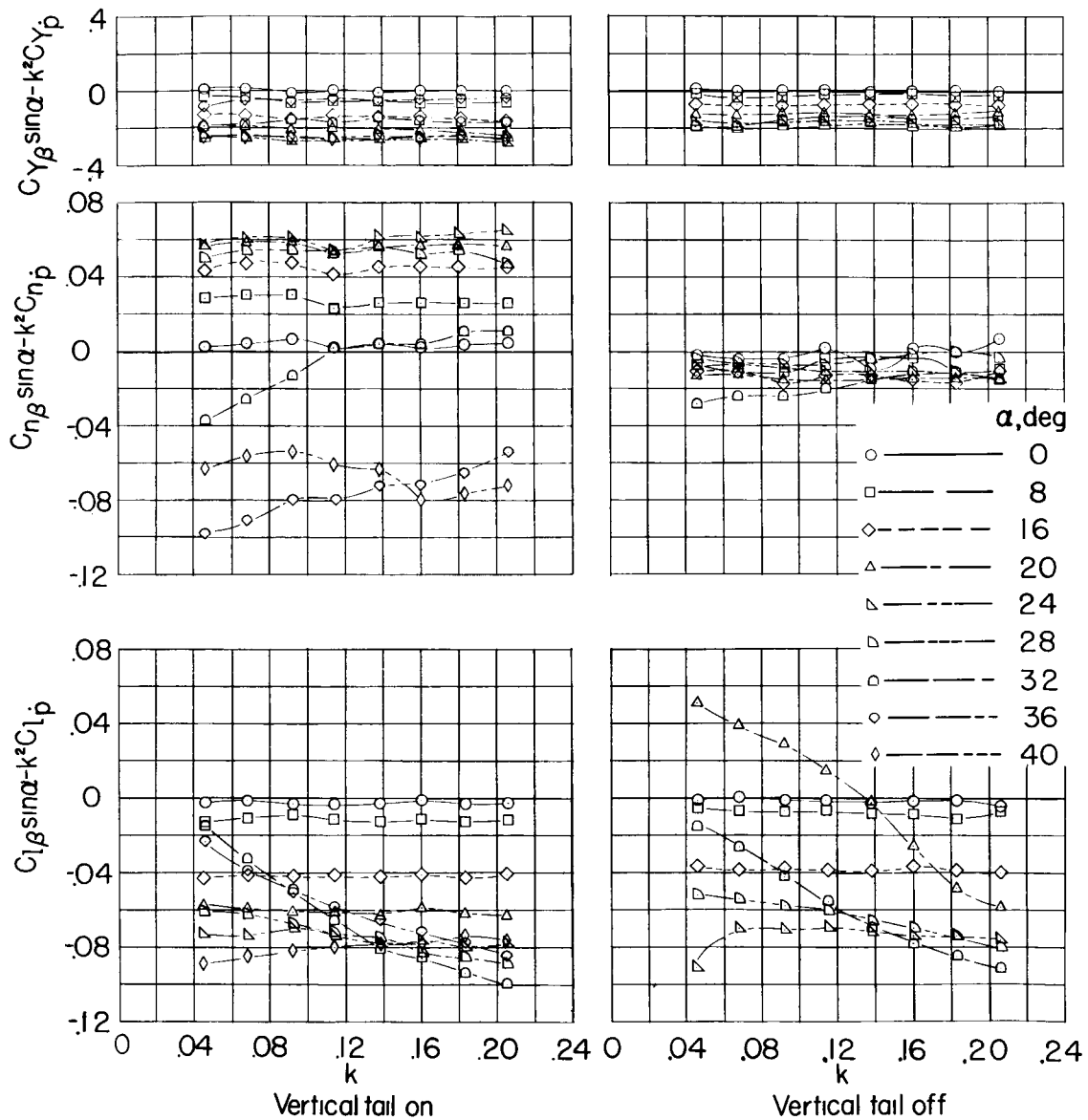


Figure 8.- Variation of in-phase rolling derivatives with frequency.
Return component.

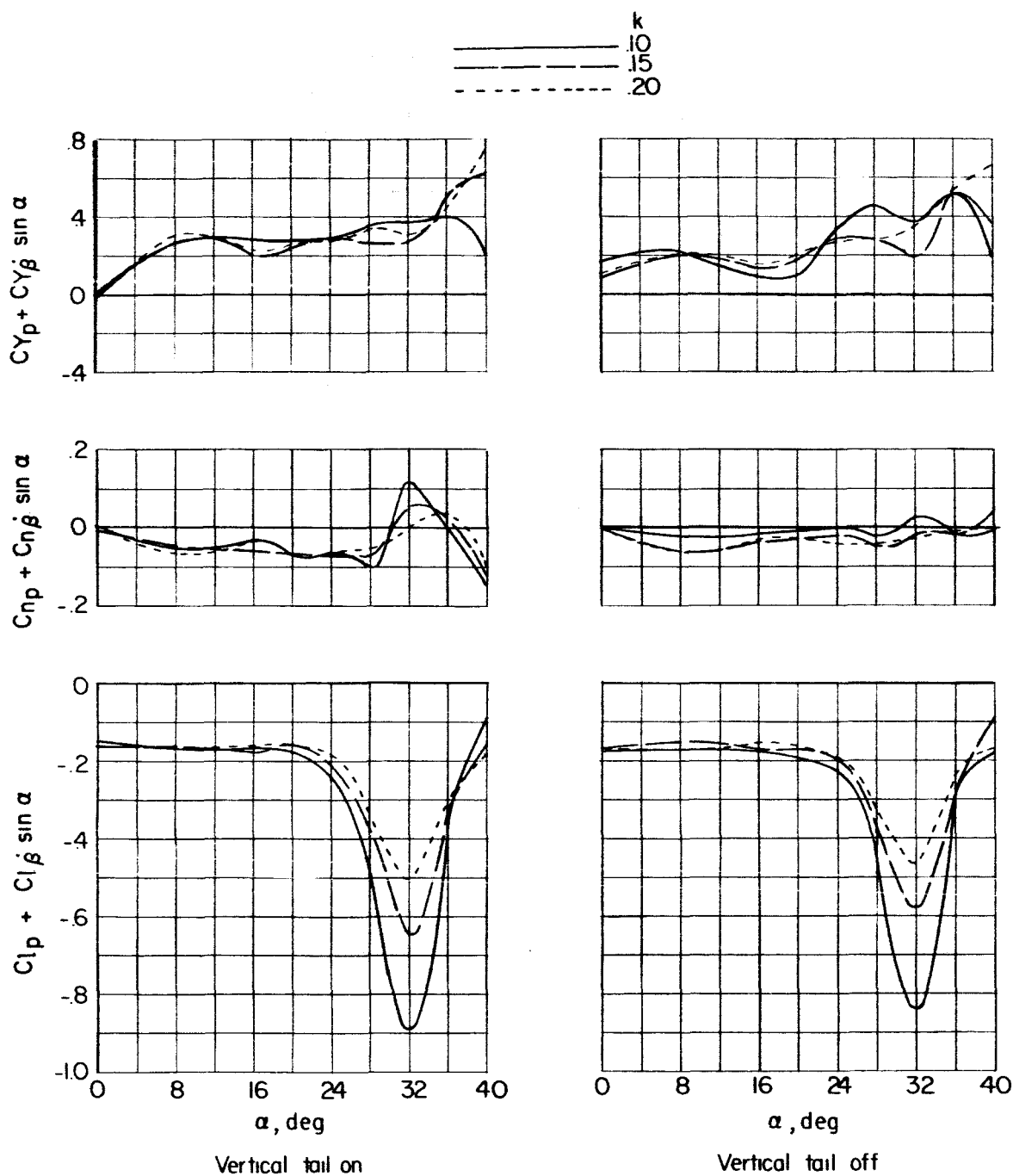


Figure 9.- Variation of out-of-phase rolling derivatives with angle of attack. Composite.

CONFIDENTIAL

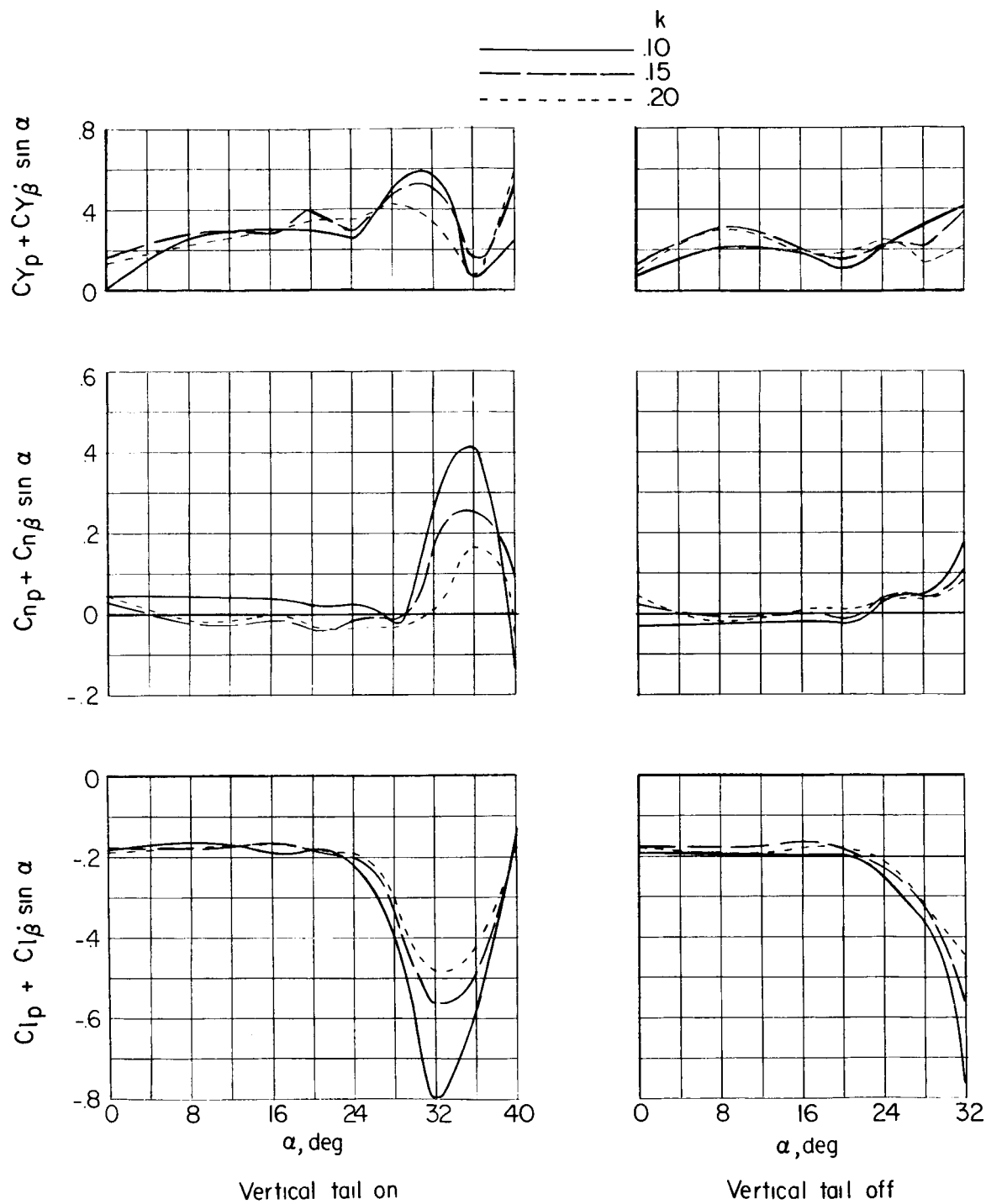


Figure 10.- Variation of out-of-phase rolling derivatives with angle of attack. Return component.

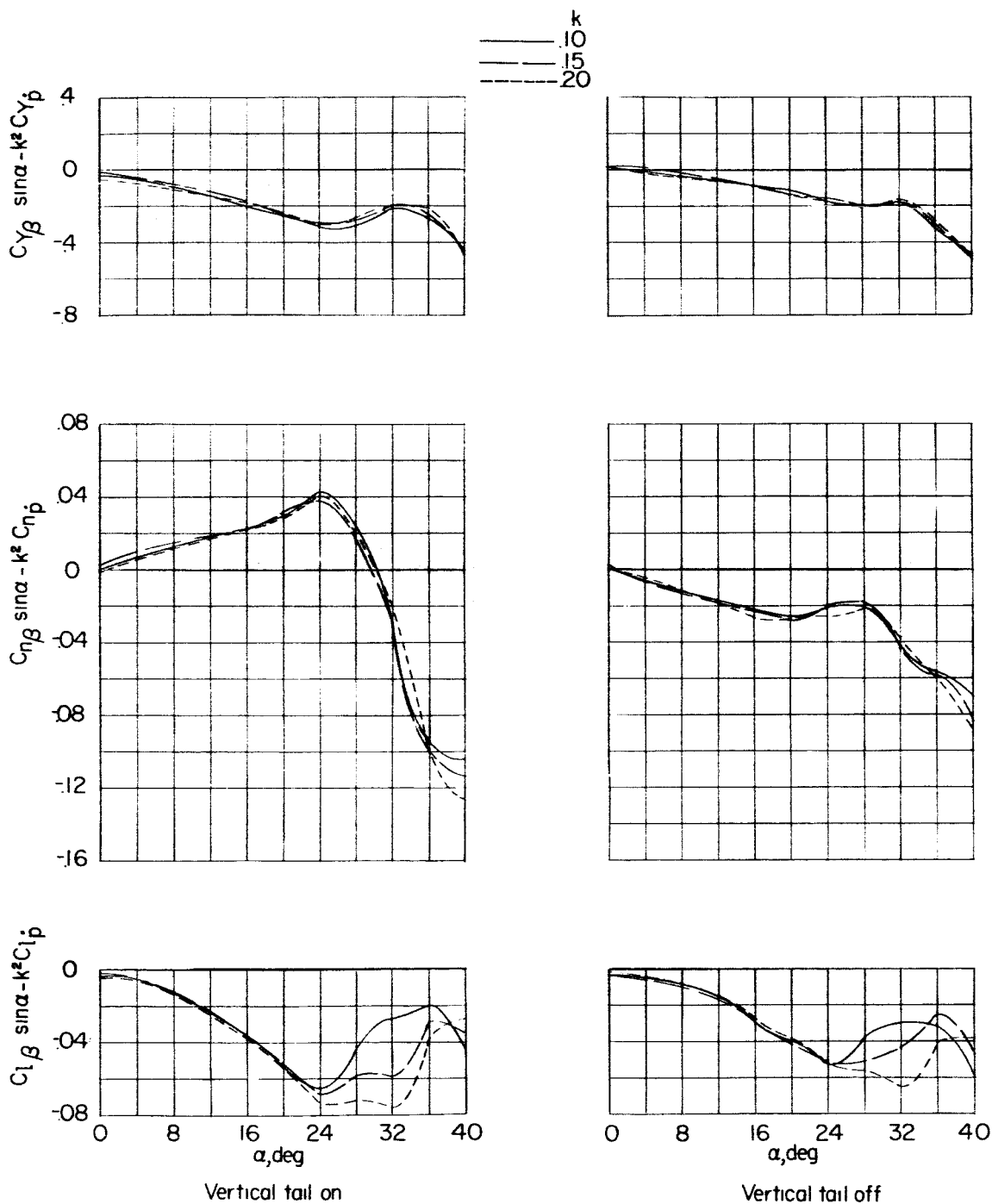


Figure 11.- Variation of in-phase rolling derivatives with angle of attack. Composite.

CONFIDENTIAL

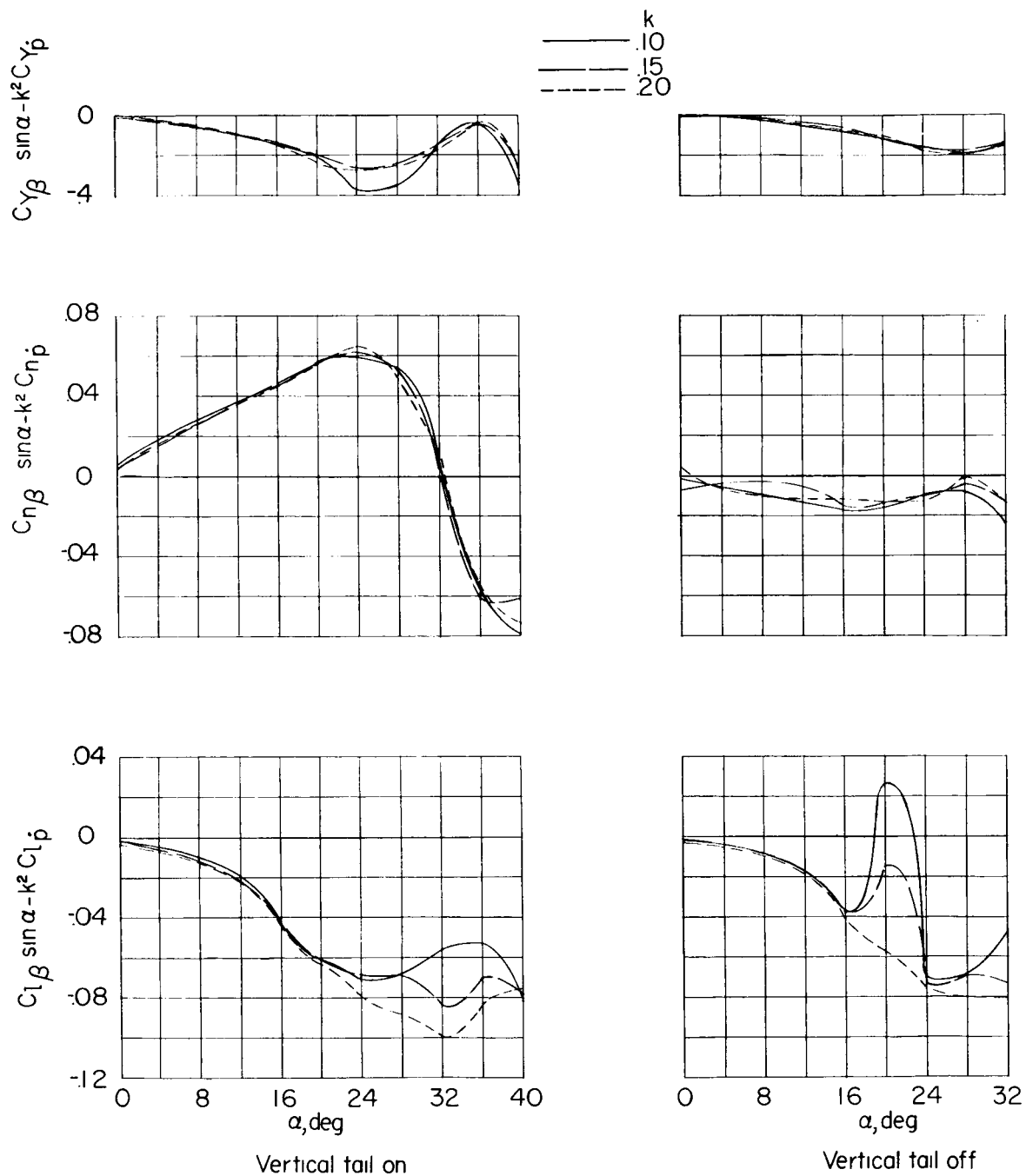
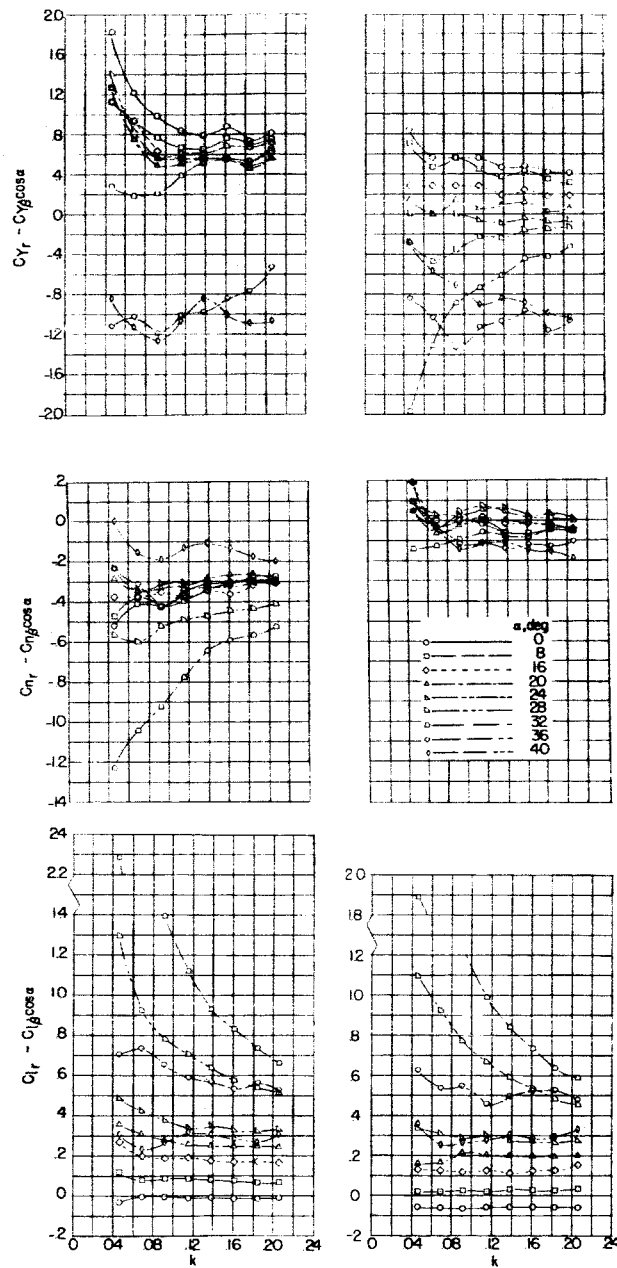


Figure 12.- Variation of in-phase rolling derivatives with angle of attack. Return component.



(a) Vertical tail on.

(b) Vertical tail off.

Figure 13.- Variation of out-of-phase yawing derivatives with frequency. Composite.

CONFIDENTIAL

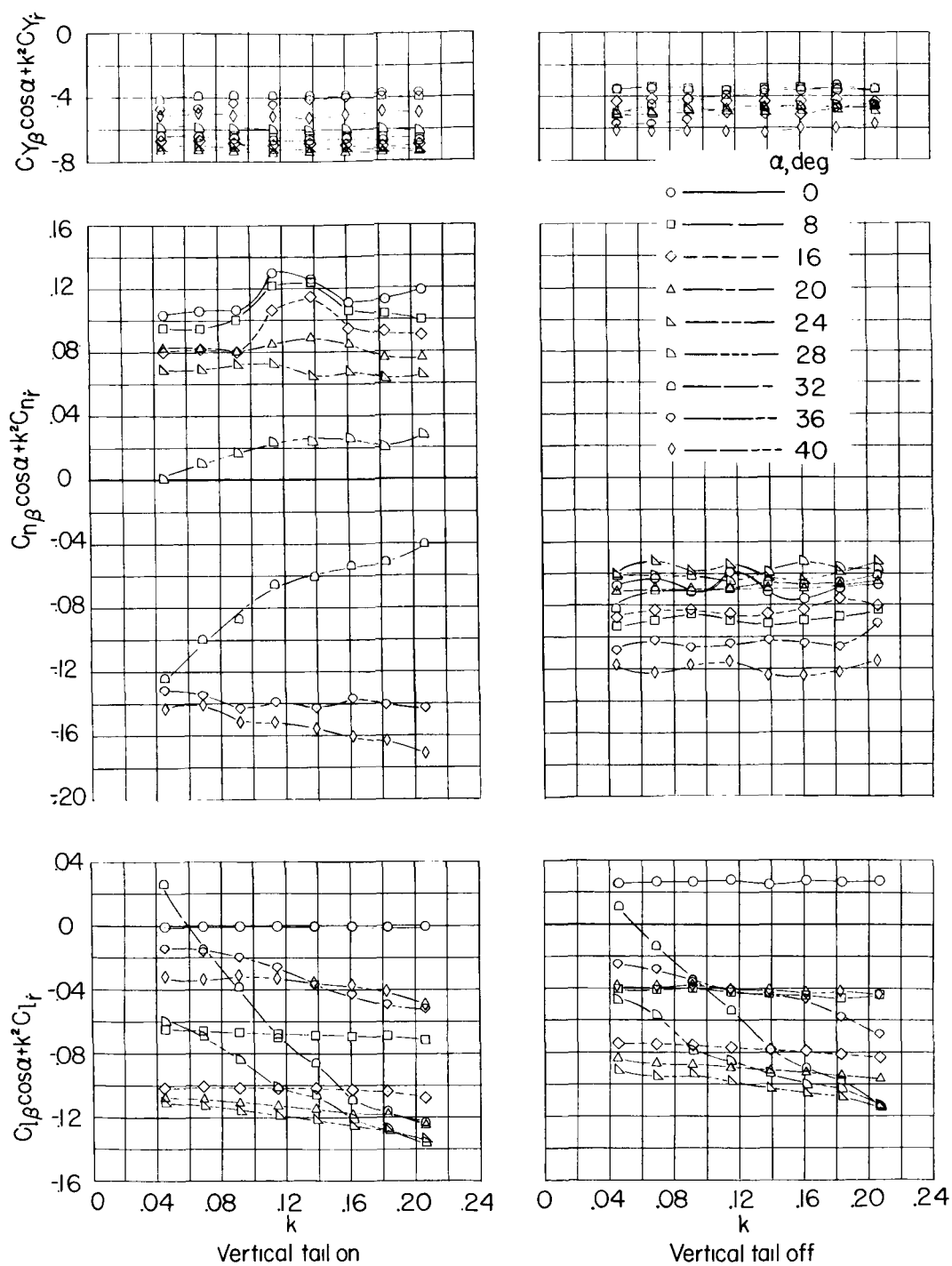
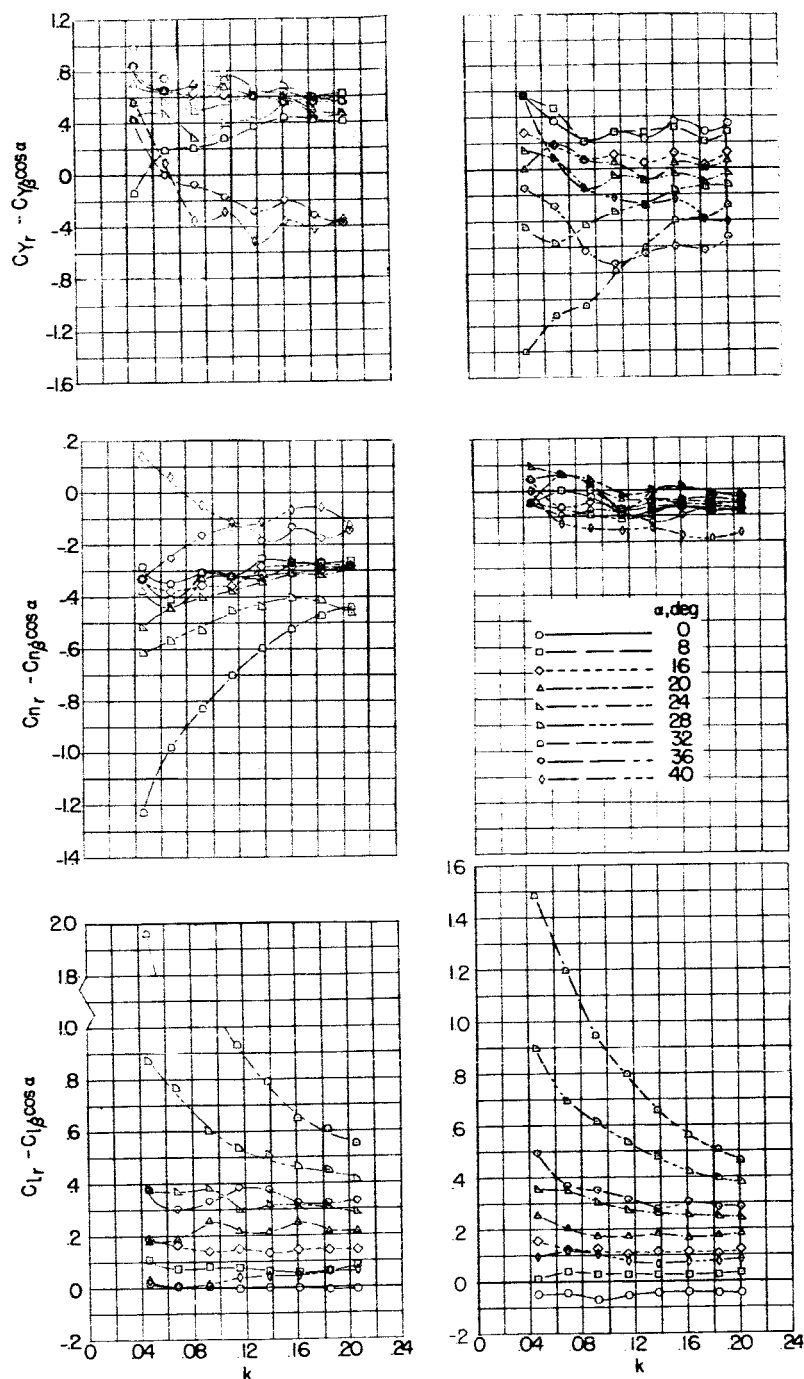


Figure 14.- Variation of in-phase yawing derivatives with angle of attack. Composite.



(a) Vertical tail on.

(b) Vertical tail off.

Figure 15.- Variation of out-of-phase yawing derivatives with frequency.
Return component.

CONFIDENTIAL

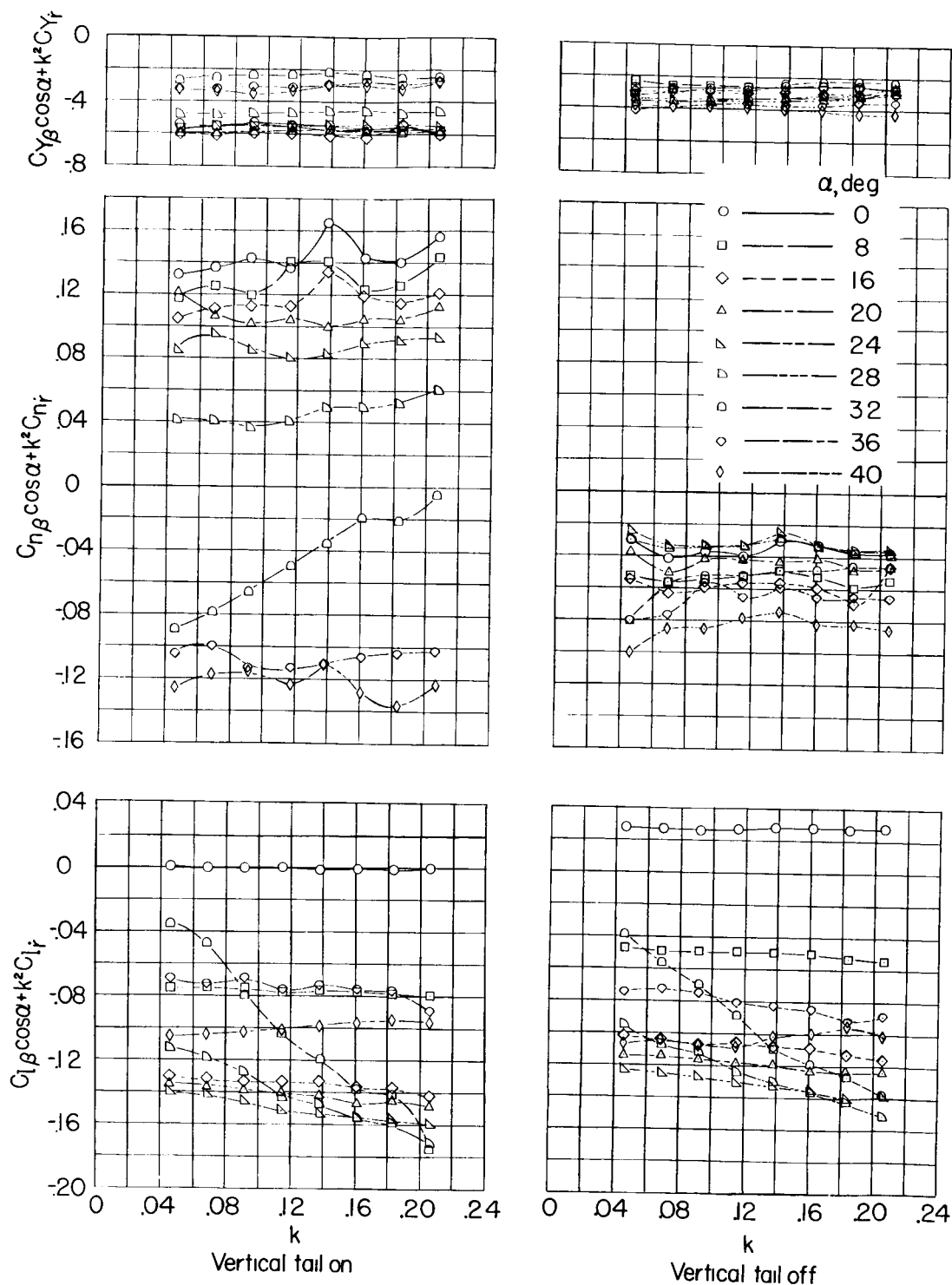


Figure 16.- Variation of in-phase yawing derivatives with frequency.
Return component.

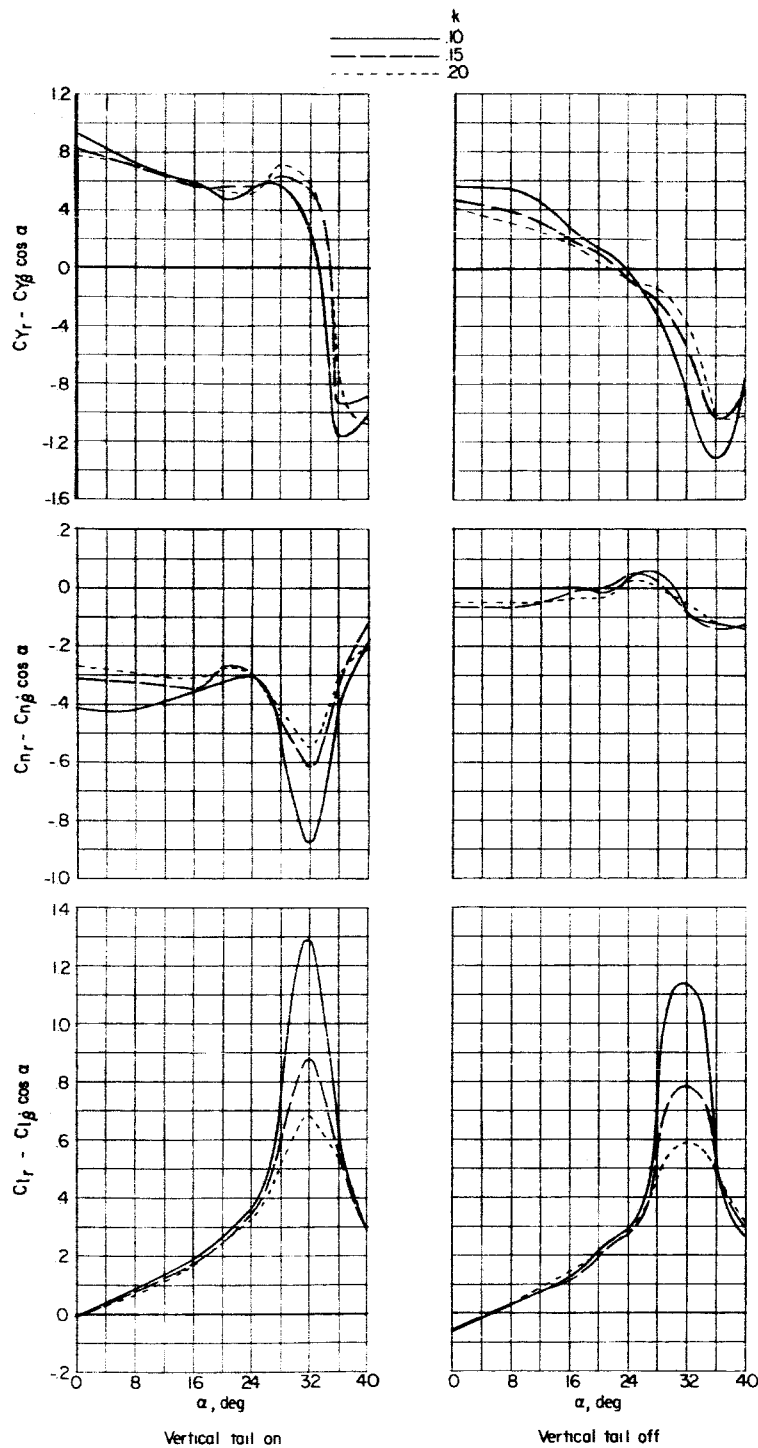


Figure 17.- Variation of out-of-phase yawing derivatives with angle of attack. Composite.

CONFIDENTIAL

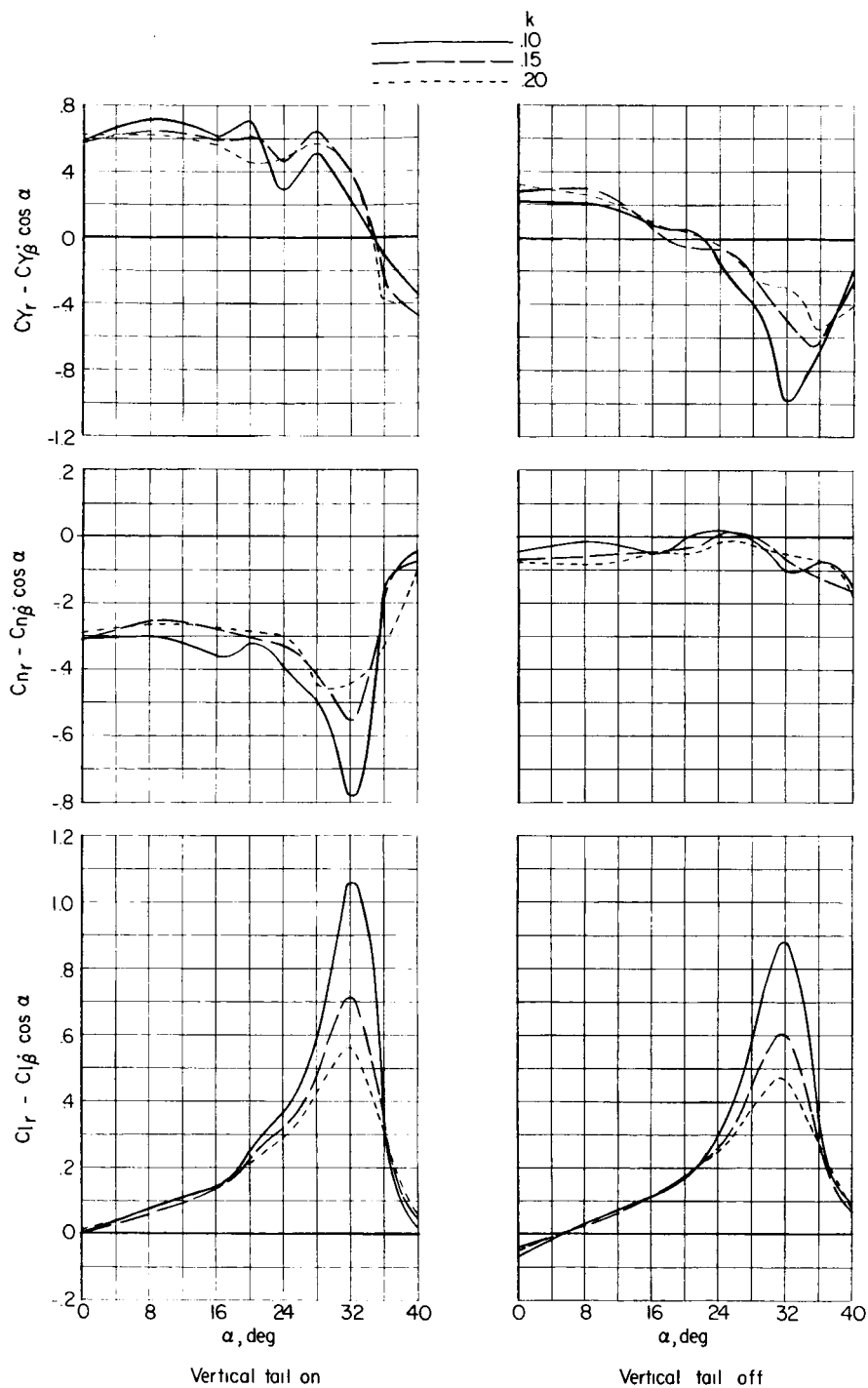


Figure 18.- Variation of out-of-phase yawing derivatives with angle of attack. Return component.

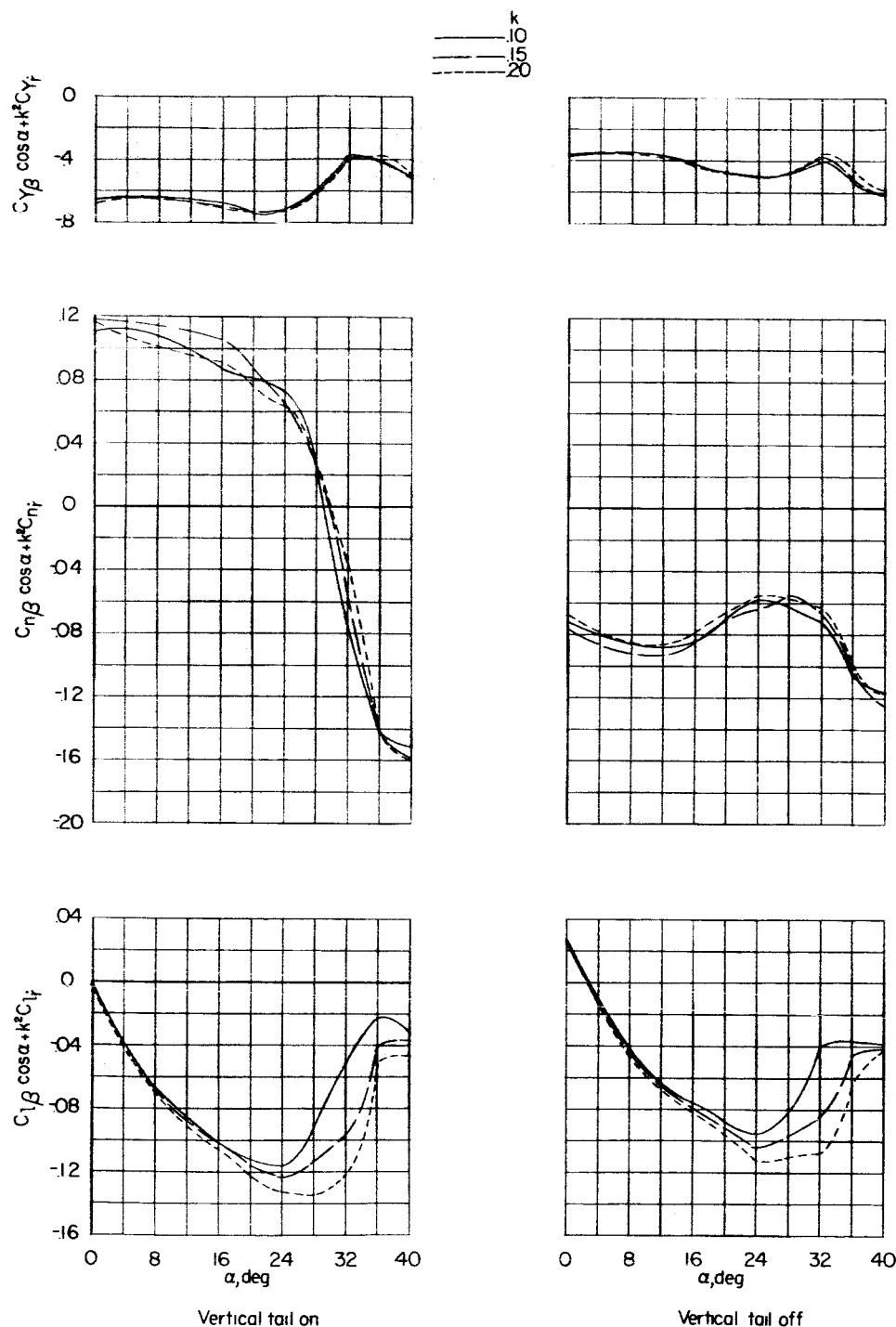


Figure 19.- Variation of in-phase yawing derivatives with angle of attack. Composite.

CONFIDENTIAL

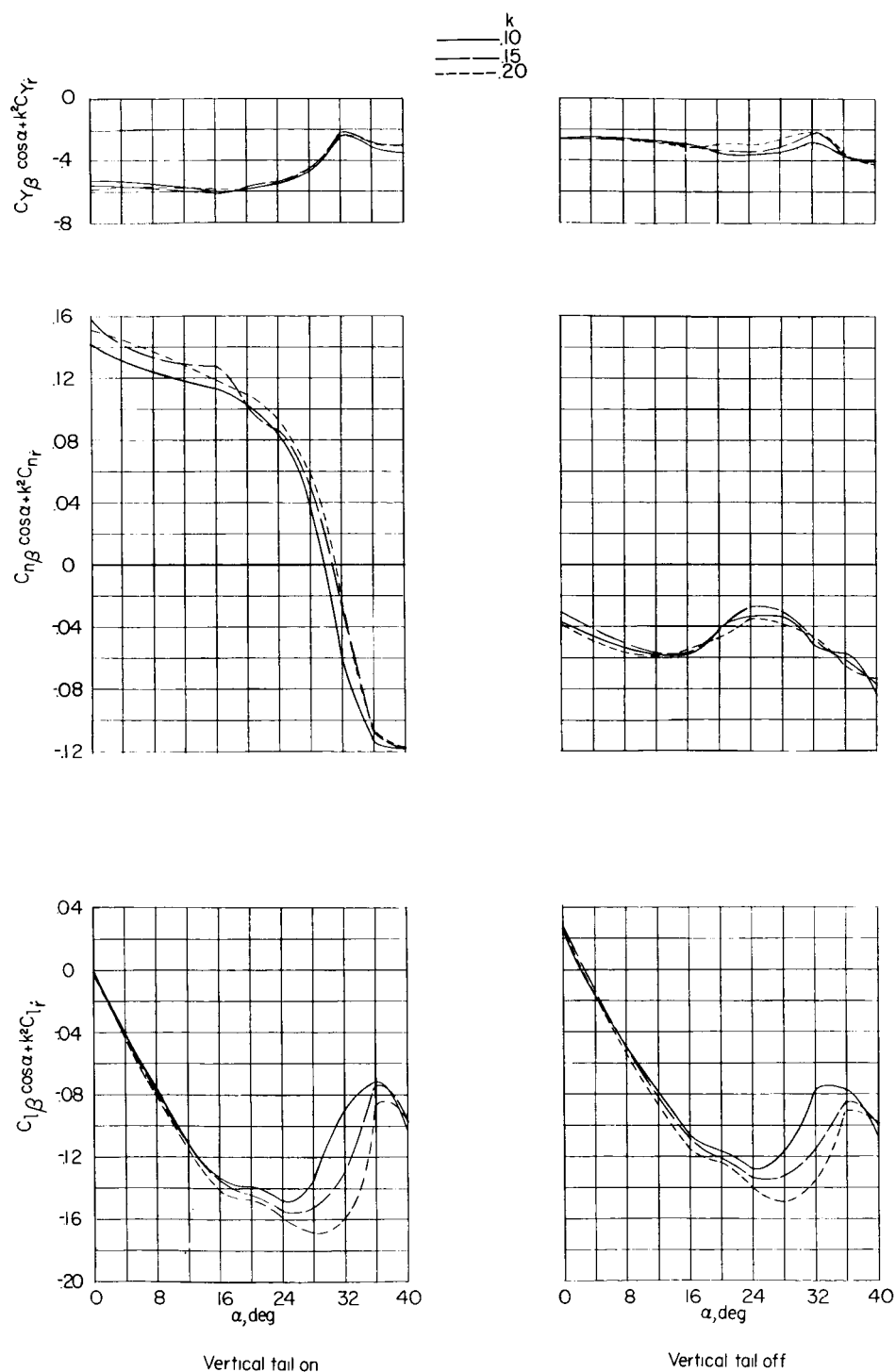
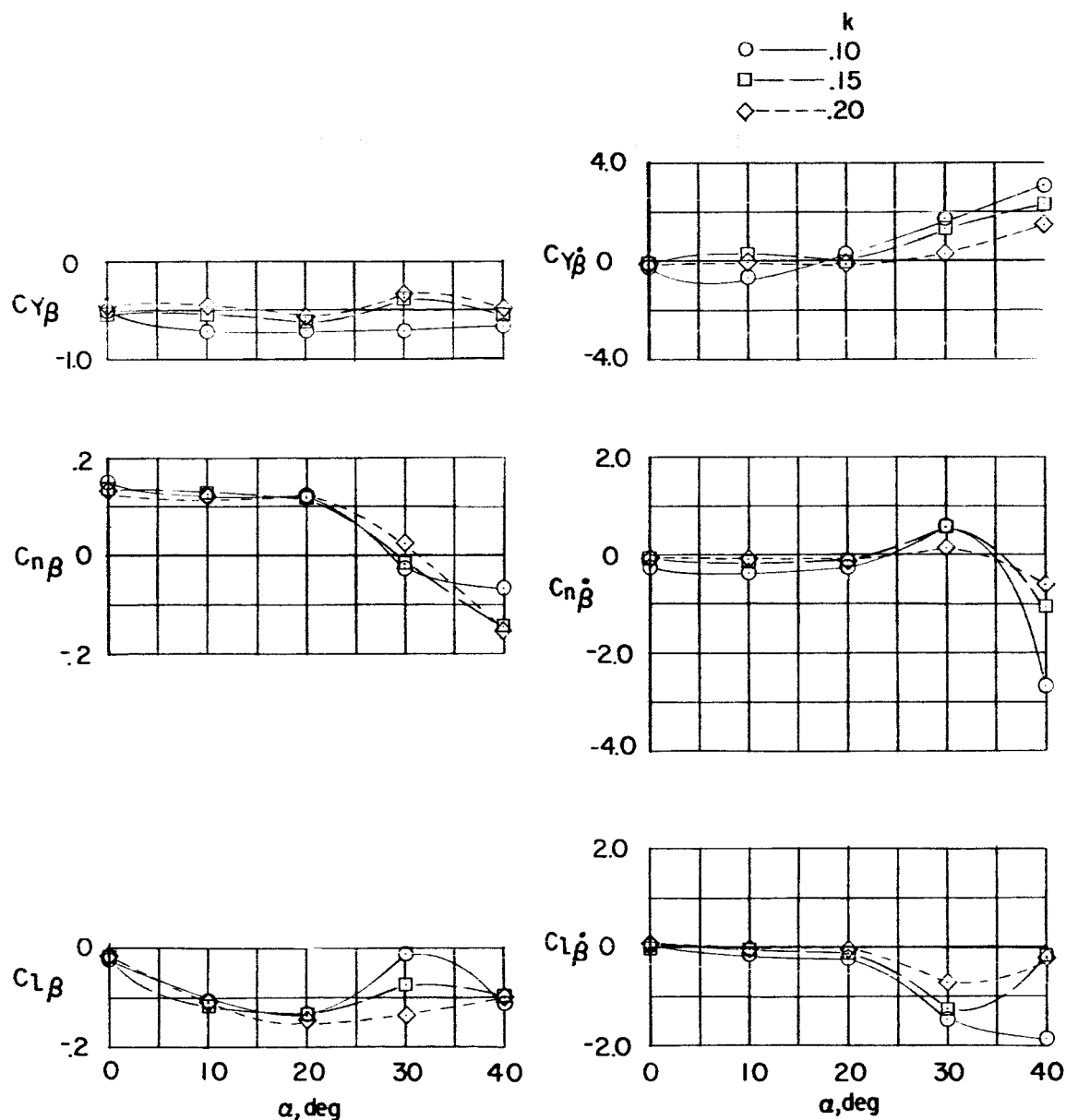


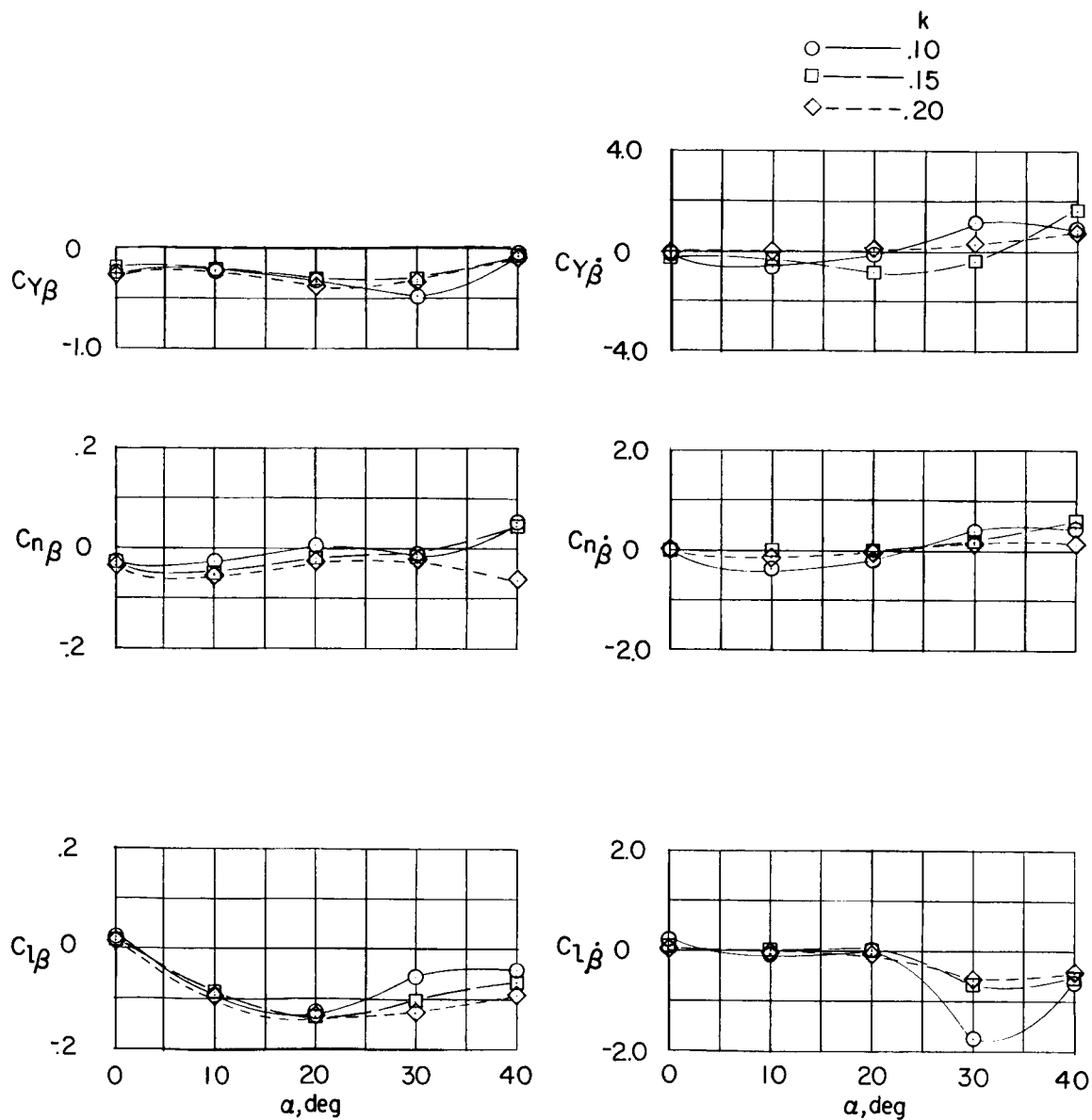
Figure 20.- Variation of in-phase yawing derivatives with angle of attack. Return component.



(a) Complete model.

Figure 21.- Variation of in-phase and out-of-phase sideslipping derivatives with angle of attack. Return component.

CONFIDENTIAL



(b) Vertical tail off.

Figure 21.- Concluded.